Estimation of spinal joint centers from external back profile and anatomical landmarks

A. Nerot [a,b,*], W. Skalli [b], X. Wang [a]

[a] Univ Lyon, Université Claude Bernard Lyon 1, IFSTTAR, UMR_T9406, LBMC, F69622 Lyon, France
[b] Institut de Biomécanique Humaine Georges Charpak, Arts et Métiers ParisTech, 75013 Paris, France

Keywords:
Joint centers prediction
External inputs
Biplanar X-rays
3D reconstruction
Subject-specific human model

A B S T R A C T

Defining a subject-specific model of the human body is required for motion analysis in many fields, such as in ergonomics and clinical applications. However, locating internal joint centers from external characteristics of the body still remains a challenging issue, in particular for the spine. Current methods mostly require a set of rarely accessible (3D back or trunk surface) or operator dependent inputs (large number of palpated landmarks and landmarks-based anthropometrics). Therefore, there is a need to provide an alternative way to estimate joint centers only using a limited number of easily palpable landmarks and the external back profile. Two methods were proposed to predict the spinal joint centers: one using only 6 anatomical landmarks (ALs) (2 PSIS, T8, C7, IJ and PX) and one using both 6 ALs and the external back profile. Regressions were established using the X-ray based 3D reconstructions of 80 subjects and evaluated on 13 additional subjects of variable anthropometry. The predicted location of joint centers showed an average error 9.7 mm (±5.0) in the sagittal plane for all joints when using the external back profile. Similar results were obtained without using the external back profile, 9.5 mm (±5.0). Compared to other existing methods, the proposed methods offered a more accurate prediction with a smaller number of palpated points. Additional methods have to be developed for considering postures other than standing, such as a sitting position.

1. Introduction

Accurate estimation of intervertebral joint centers is of primary importance to precisely define the kinematic chain of subject-specific models for posture and motion analysis. However, few solutions have been proposed to predict joint centers using easily measurable external characteristics as inputs. The geometric model in Snyder et al. (1972) has been widely used (Kennedy 1982; Choi et al., 2007; Reed et al., 1999). It provides twelve regression equations for the norm and direction of the vectors joining skin markers, located on six palpated spinous processes, to six spinal joint centers. However regressions were developed from the radiographic data of bones and surface markers of only 19 male subjects for which, to our knowledge, no validation has yet been published. Other studies proposed prediction equations using additional measurements such as anthropometric dimensions (body height and weight), L4 skinfold and difference of L1-S1 skin distraction during maximal forward bending (Lee et al., 1995; Chiou et al., 1996) in addition to palpated landmarks. However skinfold measurements might show high inter-operator variability (Klipstein-Grobusch et al., 1997; Wang et al., 2000) and accuracy may depend on skin thickness and skinfold compressibility (Himes et al., 1979). Palpation-based methods are also subject to inter-operator variation (Harlick et al., 2007) and could be time consuming if there are a high number of points to be palpated. Therefore ideally, the prediction method should require only a small number of easily palpated bony landmarks. Bryant et al. (1988) proposed an original geometric method aiming at predicting the distance between the internal spine curvature and the external back profile while using only two palpated landmarks (T1 and L5) as inputs. The curvilinear abscises of joint centers were estimated along the internal spinal profile, but the proposed method could not fully locate the spine in the sagittal plane. Moreover, only a small sample of 13 subjects from 13 to 17 years was used.

Recently a PCA-based method was proposed to predict internal pelvic landmarks and spine joint centers locations using trunk 3D surface (Nérot et al., 2016). The study was based on a database of 3D reconstructions of bones and envelopes from low dose biplanar radiographs (Dubousset et al., 2010). The main advantage is that

the proposed method requires almost no palpation. However, the full trunk skin surface is required and a scanning device is not always a standard piece of lab equipment. Furthermore, the whole trunk surface may not be easily scanned due to the obstruction by environmental objects for some applications, for example a person sitting in a seat.

Using the existing database of 3D reconstructions of both internal skeleton and external body shape used in Nérot et al. (2016), the objective of this study was to propose alternative methods for the prediction of intervertebral joint centers without using the full trunk surface scan but only a small amount of easily accessible input data.

2. Material and methods

2.1. Data

With the approval of the Ethics committee (CPP 06036) and signature of informed consents, biplane radiographs of 93 subjects were collected with a low dose EOS system (EOS Imaging, France) (46 females/47 males, age: [18, 76 years], height: [1.52, 1.97 m], weight: [45, 103 kg]). Participants were asked to adopt a free standing position (Steffen et al., 2010). These subjects were divided into two groups, a group of 80 persons for the development of the predictive methods (40 females/40 males, height: [1.52, 1.88 m], weight: [48, 103 kg]), and a second group of 13 subjects of variable anthropometry for their validation (6 females/7 males, height: [1.53, 1.97 m], weight: [45, 102 kg]). From these two radiographic views, 3D reconstruction of the lowers limbs, pelvis, spine and the external body envelope were performed (Nérot et al., 2015). Subject-specific 3D reconstructions were based on the deformation of parameterized and regionalized generic models on radiographic contours, allowing us to isolate the thoracic region (Fig. 1) and to automatically extract the following internal and external parameters:

- Internal parameters: Coordinates of 18 joint centers from C7/T1 to L5/S1, calculated as the middle points of the segments joining the barycenters of the two adjacent vertebrae end-plates (Humbert et al., 2009). The internal spine profile was approximated by a cubic spline passing through the joint centers from C7/T1 to L5/S1.
- External parameters: anatomical landmarks (ALs) on the skin surface by virtual palpation including posterior (PSIS) superior iliac spines, incisura jugularis (XJ), xiphoid process (XP) and spinous processes. Bony landmarks were extracted from the parametrized subject-specific bones models and their closest points on the envelope reconstruction were considered as an estimation of the regular palpated landmarks. The external back curvature (or back profile) was also approximated by a cubic spline passing through the spinous processes from C7 to L5 and limited at the PSIS midpoint.

2.2. Proposed predictive methods

The predictive methods proposed in the present study were similar to that of Bryant et al. (1988) (Fig. 2): firstly the internal spinal profile is predicted in a spine local coordinate system; secondly the two extreme joint centers C7/T1 and L5/S1 need to be predicted; lastly the position of all other joint centers can be located if their curvilinear coordinates are known.

The spine local coordinate system (LCS) ($\mathbf{t_0}$, **d**, **t**) in the sagittal plane was defined with the origin $\mathbf{t_0}$ at C7 palpated spinous process, **t** the axis directing from C7 to the midpoint between the two palpated PSIS (Fig. 2.1). **d** was the perpendicular axis to **t** and directed forward. The internal and external spinal profiles

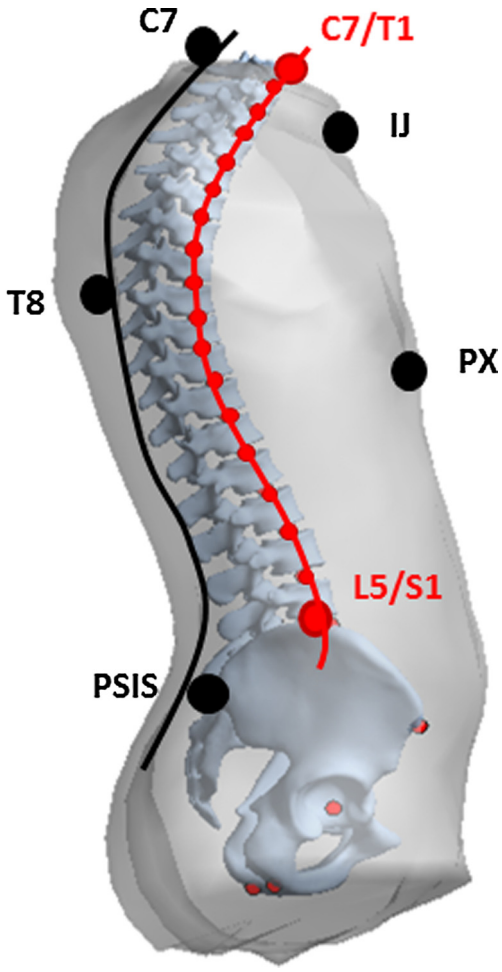

Fig. 1. Definition of external back (black) and internal spinal (red) profiles which are both approximated by a cubic spine passing through external spinal processes and internal joint centers respectively. Six palpable ALs (two PSIS, T8, C7, IJ, PX) required for the methods proposed in the present study are also illustrated. (For interpretation of the references to colour in this figure legend, the reader is referred to the web version of this article.)

were characterized by their local coordinated [d_i^{int}, t_i] and [d_i^{ext}, t_i,]. The coordinates along **t** were normalized by the distance between the midpoint of two PSIS and C7 in order to compare individuals of different corpulence.

Using the existing database, the regression equations were obtained for all variables required for predicting the internal spinal profile S^{int}, two extreme joint centers C7/T1 and L5/S1 and curvilinear coordinates of other joint centers. Two methods for predicting the internal spinal profile were proposed, one based on the distance d_i^{int} from the **t** axis, and the other based on the distance D_i (=$d_i^{int} - d_i^{ext}$) from the external back profile (Fig. 2.1).

For the internal spine profile, anthropometric dimensions (e.g. stature, weight, waist circumference etc.) and distances between ALs were searched for best predictors. Pearson tests were conducted to find the most correlated variables with D_i or d_i^{int}. For instance, based on an *a priori* assumption, thoracic depth related measurements, such as body weight, C7-IJ distance, T8-PX distance, were considered as candidate predictors. Thoracic length related parameters such as T8 to PSIS, C7 to T8 distances etc. were also considered in the Pearson test (Drerup et al., 2014). A stepwise regression method was performed on different combinations of 2 to 6 candidates to find the most powerful combination of predictors. Using the same statistical method, the t coordinates of C7/

Inputs used for methods with (and without) external back profile
Body weight, Body height
Back profile coordinates S^{ext}
Palpated ALs position: **C7, T8, IJ, PX, PSIS**
Mean point between PSIS: Mid_{PSIS}
Distances: $d_{C7\text{-}IJ}$, $d_{C7\text{-}T8}$ $d_{T8\text{-}PX}$, ($d_{T8\text{-}MidPSIS}$, $d_{C7\text{-}MidPSIS}$)
Axis **t** = **[C7-Mid_{PSIS}]**
$t_i \leftarrow$ normalized coordinates along **t**, i=[0, 0,1, ...,1]

1. Internal spine profil estimation with (left) and without (right) back profile

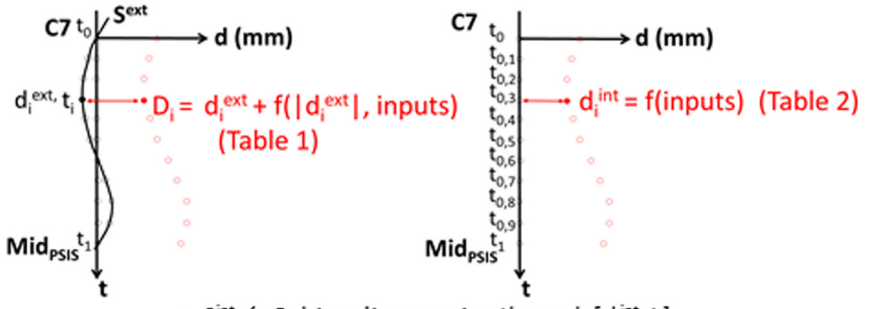

a. $S^{int} \leftarrow$ Cubic spline passing through $[d_i^{int}, t_i]$

2. C7/T1 and L5/S1 prediction

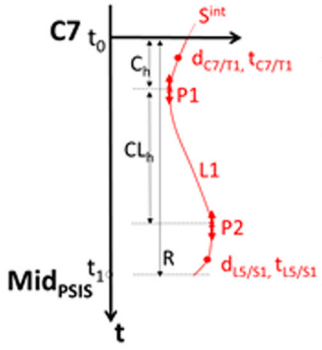

b. Locate two points P1 and P2 so that their tangents on S^{int} profile are parallel to the **t** axis

c. $t_{C7/T1} = t_0 + f(R/L1, Ch/L1, Inputs)$
$t_{L5/S1} = t_0 + f(CLh/L1, Inputs)$ (Table 3)
L1: length of the internal curve S^{int} from t_0 to t_1

d. $d_{C7/T1} = S^{int}(t_{C7/T1})$
$d_{L5/S1} = S^{int}(t_{L5/S1})$

3. T1/T2 to L4/L5 estimation using mean ratios

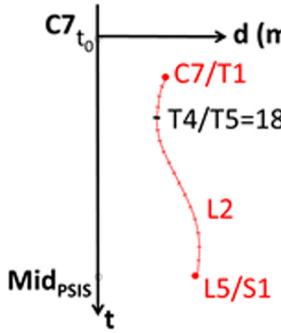

e. Return joints centers position along S^{int} (Table 4)
L2: length of the internal curve S^{int} from C7/T1 to L5/S1

Fig. 2. Successive steps for computing joint centers position using the two prediction methods.

Table 1
Regression equations (and associated RMSE errors and coefficients of determination) of the distances from the external back to the internal spinal profiles (D_i) for the 11 equally distanced points along the t axis.

D_i	Regression equations	RMSE (mm)	R^2
D_0	$0.19*d_{C7\text{-}T8} + 0.28*d_{C7\text{-}IJ} + 0.30*d_{0.6}^{ext} - 10.18$	4.8	0.7
$D_{0.1}$	$0.48*d_{C7\text{-}IJ} + 0.86*d_{0.1}^{ext} - 6.00$	4.9	0.8
$D_{0.2}$	$0.40*d_{C7\text{-}IJ} + 0.23*BW + 0.98*d_{0.2}^{ext} - 0.53*d_{0.4}^{ext} - 11.29$	5.7	0.6
$D_{0.3}$	$0.47*d_{C7\text{-}IJ} + 1.17*d_{0.3}^{ext} - 0.94*d_{0.4}^{ext} - 4.20$	6.6	0.4
$D_{0.4}$	$0.52*BW + 34.34$	6.7	0.6
$D_{0.5}$	$0.15*d_{T8\text{-}PX} + 0.34*BW + 20.45$	6.4	0.6
$D_{0.6}$	$0.17*d_{T8\text{-}PX} + 0.45*BW + 14.70$	6.5	0.6
$D_{0.7}$	$0.15*d_{T8\text{-}PX} + 0.63*BW + 12.00$	7.0	0.7
$D_{0.8}$	$0.12*d_{T8\text{-}PX} + 0.69*BW + 19.40$	6.1	0.7
$D_{0.9}$	$0.74*BW + 44.40$	6.9	0.6
D_1	$0.68*BW + 44.19$	9.3	0.4

Note: $d_{C7\text{-}IJ}$: C7 to IJ distance, $d_{i:}^{ext}$ distance of the back profile from the **t** axis at t_i, $d_{T8\text{-}PX}$: T8 to PX distance, $d_{C7\text{-}T8}$: C7 to T8 distance, body weight in kg.

Table 2
Regression equations (and associated RMSE errors and coefficients of determination) of the distances from the **t** axis to the internal spinal profiles for the 11 equally distanced points along **t**. $d_{0.3}^{int}$ is not indicated as no external predictor for $d_{0.3}^{int}$ was found by the Pearson test (mean value: 30.65 mm, RMSE, 11.6 mm).

d_i^{int}	Regression equations	RMSE (mm)	R^2
d_0	$0.19*d_{C7\text{-}T8} + 0.24*d_{C7\text{-}IJ} + 0.13*d_{T8\text{-}PX} - 25.89$	5.3	0.7
$d_{0.1}$	$0.45*d_{C7\text{-}IJ} - 5.47$	5.0	0.5
$d_{0.2}$	$0.46*d_{C7\text{-}IJ} - 0.22*d_{T8\text{-}PX} + 0.28*BW + 3.19$	7.6	0.3
$d_{0.4}$	$-0.32*d_{T8\text{-}PX} + 0.53*BW + 63.35$	11.7	0.2
$d_{0.5}$	$-2.50*d_{C7\text{-}T8} - 2.34*d_{T8\text{-}MidPSIS} + 2.42*d_{C7\text{-}MidPSIS} + 0.36*BW + 24.96$	6.7	0.7
$d_{0.6}$	$-1.95*d_{C7\text{-}T8} - 2.07*d_{T8\text{-}MidPSIS} + 2.01*d_{C7\text{-}MidPSIS} - 0.09*d_{T8\text{-}PX} + 0.58*BW + 54.81$	6.4	0.7
$d_{0.7}$	$-1.41*d_{C7\text{-}T8} - 1.67*d_{T8\text{-}MidPSIS} + 1.52*d_{C7\text{-}MidPSIS} + 0.57*BW + 65.35$	7.3	0.6
$d_{0.8}$	$-0.81*d_{C7\text{-}T8} - 1.14*d_{T8\text{-}MidPSIS} + 0.95*d_{C7\text{-}MidPSIS} + 0.70*BW + 76.41$	7.1	0.5
$d_{0.9}$	$-0.21*d_{T8\text{-}MidPSIS} + 0.84*BW + 101.58$	7.0	0.5
$d_{1.0}$	$-0.16*d_{C7\text{-}MidPSIS} + 1.00*BW + 99.61$	8.5	0.5

Note: $d_{C7\text{-}IJ}$: C7 to IJ distance, $d_{T8\text{-}PSIS}$: distance bewteenT8 and PSIS midpoint, $d_{C7\text{-}PSIS}$: distance between C7 and PSIS midpoint, $d_{T8\text{-}PX}$: T8 to PX distance, $d_{C7\text{-}T8:}$ C7 to T8 distance.

Table 3
Predictors and regression coefficients to predict the spine extremities C7/T1 and L5/S1 from spine shape descriptors.

	Regression equations	RMSE (mm)	r^2
$t_{C7/T1}$	$-(-1.02*R + 0.07*Ch + 0.99)*R$	10.5	0.5
$t_{L5/S1}$	$-(0.49*CL_h + 0.92)*R$	18.3	0.4

Note: R, C_h and CL_h are described in Fig. 2.2

Table 4
Mean position of intervertebral joint centers along S^{int} normalized by the developed length of internal spline from C7/T1 and L5/S1. Standard errors in percentage and mm are indicated.

	Mean	SD (%)	SD (mm)
C7/T1	0	0	0
T1/T2	4	0	1.57
T2/T3	9	1	2.4
T3/T4	13	1	3.11
T4/T5	18	1	3.13
T5/T6	23	1	3.54
T6/T7	28	1	3.94
T7/T8	33	1	4.23
T8/T9	38	1	4.52
T9/T10	43	1	4.83
T10/T11	49	1	4.75
T11/T12	55	1	4.76
T12/L1	61	1	4.69
L1/L2	69	1	4.68
L2/L3	76	1	4.68
L3/L4	84	1	4.46
L4/L5	92	0	2.99
L5/S1	100	0	1.82

T1 and L5/S1 along the 2D spinal profile were supposed to be dependent on S^{int} curvature descriptors (Fig. 2.2). Finally, the mean curvilinear coordinates of joint centers were calculated to estimate the relative position of joint centers along the internal spine estimate S^{int} (Fig. 2.3).

2.3. Evaluation

Root mean square errors (RMSE) were calculated between estimated (regression) and reference (EOS based reconstructions) joint centers coordinates in the sagittal plane to assess the two proposed predictive methods. First, the data from 80 subjects, from which the regression equations were obtained, were used. Then an additional sample of 13 subjects was also considered for validation.

3. Results

3.1. Internal spine profile prediction

Up to eleven equal-distanced points along C7 to PSIS axis (t axis, Fig. 2.1), with t = [0, 0.1, . . . ,1], were used to characterize both external and internal spine profiles. Tables 1 and 2 provide the predictors for d_i^{int} and D_i. The distance D_i from the external back profile showed smaller RMS errors than the distance d_i^{int} from the t axis.

3.2. C7/T1 and L5/S1 prediction

The regression equations to predict the vertical distance $t_{C7/T1}$ and $t_{L5/S1}$ from t_0 on S^{int} are listed in Table 3. Estimation of $t_{L5/S1}$

Table 5
Root mean square errors (RMSE) in x (antero-posterior), y (medio-lateral) and the 2D distance between reference and estimated joint centers using methods with or without using the external back profiles (mm) on the training group of 80 subjects. Standard deviations are provided.

	Using the external back profile				Without using the external back profile			
	2D distance RMSE				2D distance RMSE			
	x	y	Mean	SD	x	y	Mean	SD
C7/T1	6.8	5.5	8.7	4.5	4.0	5.5	6.8	3.5
T1/T2	4.7	5.6	7.3	3.3	4.7	5.1	6.9	3.2
T2/T3	5.1	5.7	7.7	3.3	5.5	4.8	7.4	3.6
T3/T4	5.4	5.8	7.9	3.4	6.8	4.7	8.2	4.1
T4/T5	5.8	5.7	8.2	3.6	7.7	4.5	8.9	4.5
T5/T6	6.3	6.1	8.8	3.8	8.9	4.7	10.0	4.7
T6/T7	6.7	6.4	9.3	4.1	9.8	4.9	11.0	5.1
T7/T8	6.8	6.6	9.5	4.4	9.8	5.1	11.1	5.2
T8/T9	6.8	6.8	9.6	4.7	8.9	5.2	10.3	5.1
T9/T10	6.8	7.0	9.8	5.0	7.5	5.5	9.3	4.7
T10/T11	6.8	7.1	9.8	5.2	6.6	5.8	8.8	4.5
T11/T12	6.9	7.2	10.0	5.4	6.2	6.1	8.8	4.5
T12/L1	7.0	7.6	10.3	5.8	6.3	6.7	9.2	4.7
L1/L2	7.2	8.2	10.9	6.1	6.9	7.4	10.2	5.4
L2/L3	6.9	9.0	11.3	6.1	7.4	8.2	11.0	6.0
L3/L4	6.0	9.3	11.1	5.4	7.4	8.2	11.0	6.0
L4/L5	6.7	9.8	11.9	5.6	6.7	9.1	11.3	5.6
L5/S1	8.0	9.9	12.7	5.9	7.2	9.5	11.9	5.3
Total			9.7	5.5			9.5	5.0

Note: Equations showing larger RMS errors ($D_{0.3}$, $D_{0.4}$, $D_{0.7}$ in Table 1, and d0.3int, d0.4int, d0.7int in Table 2) were not used for the least square estimation of the internal spine S^{int}.

Table 6
Mean error on 3D distance and standard error (SD) between estimated end reference joint centers on the validation group of additional 13 subjects (mm) using the back profile. A third orthogonal axis was added to the 2D local system and additional medio-lateral joint coordinates were supposed to be aligned with the **t** axis so that joint i was located with respectively (**d**,0,**t**) antero-posterior, medio-lateral and vertical coordinates.

	Mean	SD
C7/T1	7.0	3.9
T1/T2	9.5	5.4
T2/T3	11.5	5.9
T3/T4	10.7	6.6
T4/T5	9.6	6.2
T5/T6	9.5	5.7
T6/T7	10.0	5.8
T7/T8	10.6	5.8
T8/T9	10.3	5.5
T9/T10	9.5	5.1
T10/T11	8.8	5.9
T11/T12	9.7	5.7
T12/L1	10.4	5.3
L1/L2	11.2	5.0
L2/L3	11.5	5.3
L3/L4	12.1	5.9
L4/L5	10.9	6.4
L5/S1	10.6	5.7
Total	10.2	5.6

showed a higher error than $t_{C7/T1}$. $d_{C7/T1}$ and $d_{L5/S1}$ were defined at the intersection on S^{int} at $t_{C7/T1}$, and $t_{L5/S1}$, respectively.

3.3. Mean curvilinear coordinates of the joint centers

The relative positions (curvilinear abscises normalized by the curvature length) of the joint centers along the internal spinal profile were observed to be quite invariant among the subjects (SD < 5 mm, Table 4).

3.4. Evaluation

The 2D distance between estimated and reference joint centers using both methods showed very similar errors, respectively 9.7 mm (±5.0) and 9.5 mm (±5.0) with or without using the external back profile (Table 5).

As the most precise regression equations were found with the method using the external back profile (Table 1), this method was applied for predicting each joint centers location over the validation cohort of 13 subjects. Mean error was 10.2 ± 5.6 mm (Table 6).

4. Discussion

Two methods requiring a small amount of easily accessible inputs to predict all of the thoracic and lumbar intervertebral joint centers locations were compared. A focus was given to the sagittal plane where the main variations in spine shape occur for asymptomatic subjects. Only small differences were obtained between the two methods, either using only 6 ALs or using both 6 ALs and the external back profile.

Both methods were able to predict all of the 18 thoracic and lumbar joint centers while most existing geometrical models are usually able to predict only lumbar joint centers (Sicard and Gagnon, 1993; Lee et al., 1995; Chiou et al., 1996) or a few joints, e.g. C2/C3, C7/T1, T4/T5, T8/T9, T12/L1, L2/L3 and L5/S1 (Snyder et al., 1972). The mean error of 10.2 ± 5.6 mm was lower than the PCA-based method in Nérot et al., 2016 (12.8 ± 5.0 mm). This might be due to the pre-selection phase of candidate predictors at the areas with thinner layers of soft tissues. Conversely the PCA method took into account the entire trunk surface and associated shape variation, like in the belly region, which are probably independent of spine joint locations.

An extension of Snyder et al.'s method for all joint centers was also considered. This alternative method requires the estimation of 2 unknowns for each joint: the distance to its orthogonal projection on the back profile and the curvilinear abscissa of this projection. However greater prediction errors may result from the larger number of unknowns. Moreover normal vectors to the back surface were barely reproducible depending on the quality of acquisition and the smoothing method. The advantages of the current methods are to estimate a smaller number of unknown variables and to

robustly define a unique direction for calculating the spine coordinates in the sagittal plane.

L5/S1 estimates using only C7 and PSIS landmarks showed a higher error compared to the PCA method in Nérot et al. (2016) using the whole trunk surface including the pelvic region. This might highlight the importance of considering some pelvic anatomical descriptors for the L5/S1 prediction. For example, a simple method for predicting the L5/S1 from pelvic landmarks was proposed in Peng et al., 2015. Joint location errors were reduced by 1 to 5 mm on average when considering our methods and imposing the true position of L5/S1. This confirms the importance of an accurate prediction of L5/S1 position to precisely locate the rest of the spinal joints.

The major limitation of this method is that it is based on a standing posture and may not be applicable to alternative postures involving different spinal curvatures (such as sitting or supine). Furthermore, as virtual palpation was performed, the influence of palpation errors on these regression methods needs to be tested on a cohort of volunteers in future work.

5. Conclusion

This study proposed two geometric models allowing the prediction of spine joint centers from C7/T1 to L5/S1 with much less data than existing methods while concurrently improving the precision of the predictions. The methods are adapted to current methodology in motion analysis and applicable with minimal lab equipment. Prediction of L5/S1 using predictors from the pelvis could improve the results. Work is ongoing to change the standing position to a desired posture such as a seated position in order to enlarge the possibility of applications.

Acknowledgements

The authors thank the ParisTech BiomecAM chair program on subject-specific musculoskeletal modeling, and in particular COVEA and Société Générale, as well as IFSTTAR for the PhD grant.

Conflict of interest statement

We hereby declare there are no financial or personal relationships with other people or organizations that could inappropriately influence (bias) this work.

References

Bryant, J.T., Gavin, J., Smith, B.L., Stevenson, J.M., Reid, J.G., Smith, B.L., Stevenson, J. M., 1988. Method for determining vertebral body positions in the sagittal plane using skin markers. Spine 14 (3), 258–265.

Chiou, W.K., Lee, Y.H., Chen, W.J., Lee, M., Lin, Y.H., 1996. A non-invasive protocol for the determination of lumbar spine mobility. Clin. Biomech. 11 (8), 474–480.

Choi, H.Y., Kim, K.M., Han, J., Sah, S., Kim, S.H., Hwang, S.H., Lee, K.N., Pyun, J.K., Montmayeur, N., Marca, C., Haug, E., Lee, I., 2007. Human body modeling for riding comfort simulation. In: Duffy, V.G. (Ed.), Digital Human Modeling. ICDHM 2007. Lecture Notes in Computer Science. Springer, Berlin, Heidelberg.

Drerup, B., 2014. Rasterstereographic measurement of scoliotic deformity. Scoliosis 9 (1), 22.

Dubousset, J., Charpak, G., Skalli, W., Deguise, J., Kalifa, G., 2010. Eos: a new imaging system with low dose radiation in standing position for spine and bone & joint disorders. J. Musculoskeletal Res. 13 (01), 1–12.

Harlick, J.C., Milosavljevic, S., Milburn, P.D., 2007. Palpation identification of spinous processes in the lumbar spine. Manual Therapy 12 (1), 56–62.

Himes, J.H., Roche, A.F., Siervogel, R.M., 1979. Compressibility of skinfolds and the measurement of subcutaneous fatness. Am. J. Clin. Nutr. 32, 1734–1740.

Humbert, L., De Guise, J.A., Aubert, B., Godbout, B., Skalli, W., 2009. 3D reconstruction of the spine from biplanar X-rays using parametric models based on transversal and longitudinal inferences. Med. Eng. Phys. 31 (6).

Kennedy, K.W., 1982. Workspace Evaluation and Design: USAF Drawing Board Manikins and the Development of Cockpit Geometry Design Guides, Anthropometry and Biomechanics: Theory and Application. Plenum Press, New York, USA, pp. 205–213.

Klipstein-Grobusch, K., Georg, T., Boeing, H., 1997. Interviewer variability in anthropometric measurements and estimates of body composition. Int. J. Epidemiol. 26 (Suppl 1), S174–S180.

Lee, Y.H., Chiou, W.K., Chen, W.J., Lee, M.Y., Lin, Y.H., 1995. Predictive model of intersegmental mobility of lumbar spine in the sagittal plane from skin markers. Clin. Biomech. 10 (8), 413–420.

Nérot, A., Skalli, W., Wang, X., 2016. A principal component analysis of the relationship between the external body shape and internal skeleton for the upper body. J. Biomech. 49 (14), 3415–3422.

Nérot, A., Choisne, J., Amabile, C., Travert, C., Pillet, H., Wang, X., Skalli, W., 2015. A 3D reconstruction method of the body envelope from biplanar X-rays: evaluation of its accuracy and reliability. J. Biomech. 48 (16).

Peng, J., Panda, J., Van Sint Jan, S., Wang, X., 2015. Methods for determining hip and lumbosacral joint centers in a seated position from external anatomical landmarks. J. Biomech. 48 (2), 396–400.

Reed, M.P., Manary, M.A., Schneider, L.W., 1999. Methods for measuring and representing automobile occupant posture. SAE Int. 108 (724), 1–14.

Sicard, C., Gagnon, M., 1993. A geometric model of the lumbar spine in the sagittal plane. Spine 18 (5), 646–658.

Snyder, R.G., Chaffin, D.B., Schutz, R.K., 1972. Link system of the human Torso. Aerospace Medical Research Laboratory, Wright-Patterson Air Force base. Ohio.1972 n.p. 41 (3), 1974.

Steffen, J.S., Obeid, I., Aurouer, N., Hauger, O., Vital, J.M., Dubousset, J., Skalli, W., 2010. 3D postural balance with regard to gravity line: an evaluation in the transversal plane on 93 patients and 23 symptomatic volunteers. Eur. Spine J. 19 (5), 760–767.

Wang, J., Thornton, J.C., Kolesnik, S., Pierson, R.N., 2000. Anthropometry in body composition. an overview. Ann N Y Acad Sci. 904, 317–326.